Int. J. Environ. Sci. Technol. (2014) 11:1887–1896
DOI 10.1007/s13762-013-0392-z

ORIGINAL PAPER

Modeling chromium(VI) reduction by *Escherichia coli* 33456 using ceramic pearl as a supporting medium

Y.-H. Lin

Received: 29 May 2012 / Revised: 14 May 2013 / Accepted: 9 October 2013 / Published online: 30 October 2013

Abstract A mathematical model was developed to describe the reduction of Cr(VI) by *Escherichia coli* (*E. coli*) 33456 in a fixed biofilm reactor. A laboratory-scale column reactor was conducted to verify the model system. The batch kinetic tests were independently conducted to determine the biokinetic parameters used in the model simulation. With the assumed values of initial biofilm thickness (L_{f0}), the mathematical model simulated well the experimental results for Cr(VI) effluent concentration, effluent concentration of suspended *E. coli* cells, and Cr(III) production. The concentration of suspended *E. coli* cells reached up to 1.2 mg cell/L while the thickness of attached *E. coli* cells was estimated to be 32.6 μm at a steady-state condition. At the steady state, the removal efficiency of Cr(VI) was about 92 % and the effluent concentration of Cr(III) was approximately 1.6 mg/L. The approaches presented in this study can be employed for the design of a pilot-scale or full-scale fixed biofilm reactor to treat Cr(VI)-containing wastewater.

Keywords Reduction · Chromium(VI) · Chromium(III) · Batch test · Continuous-flow column test · Kinetic model

Introduction

Chromium ions occur infrequently in nature, and their presence in soil and water is generally the result of industrial and domestic discharges (Lazaridis and Charalambous 2005; Kanmani et al. 2012). Like all transition metals, chromium can exist in several oxidation states ranging from Cr(0), the metallic form, to Cr(VI), the hexavalent form (Baran et al. 2007). Only the trivalent and hexavalent forms are environmentally important, the latter being of particular concern because of its greater toxicity (Goyal et al. 2003). Moreover, chromium is found in the environment mostly as hexavalent chromium(VI) (Cr(VI)). Cr(VI) is classified by the US EPA as a group A carcinogen based on its chronic and subchronic effects (Yassi and Nieboer 1988). Effects of chronic exposure to Cr(VI) include dermatitis, skin ulceration, and chromosome aberrations. Cr(VI) often originate from such industrial sources as dyes and pigments, leather tanning, photographic film-making, wood preservation, metal cleaning, car manufacturing, petroleum refining, galvanometry and electric, and agriculture activity (Nkhalambayausi-chirwa and Wang 2001; Baran et al. 2007). Thus, Cr(VI) removal has gained a great attention in water and wastewater treatment processes.

Conventional chemical treatment involves reduction of Cr(VI) to Cr(III) by adding a reducing agent under low pH (2–3) conditions and subsequent adjustment of solution pH to near-neutral pH ranges to precipitate Cr(III). Unlike the conventional chemical treatment methods for Cr(VI) reduction, biological treatment processes do not require the addition of costly chemical agents for pH adjustment and, therefore, may provide an attractive alternative to the existing technique for Cr(VI) removal (Wang and Chirwa 1998). The ability of some microorganisms to reduce highly soluble and toxic Cr(VI) to less toxic and soluble Cr(III) has been reported (Lovley and Phillips 1994; Wang and Xiao 1995). *E. coli* cells reduced Cr(VI) under both aerobic and anaerobic conditions as described in the earlier study by Wang and Shen (1997). They demonstrated

Y.-H. Lin (✉)
Department of Safety, Health and Environmental Engineering, Central Taiwan University of Science and Technology, 666, Bu-zih Road, Bei-tun District, Taichung 40601, Taiwan
e-mail: yhlin1@ctust.edu.tw

Cr(VI) reduction by Cr(VI)-reducing organism, *E. coli* ATCC 33456 in the batch tests. However, relatively few efforts have been directed toward the development of fixed biofilm process to treat Cr(VI)-containing wastewater, mainly due to insufficient knowledge about the kinetics of Cr(VI) reduction from a non-steady-state to a steady-state condition in a continuous-flow fixed biofilm process.

To optimize the design and operation of fixed biofilm process for Cr(VI) reduction, a thorough understanding of the kinetic characteristics of microbial transformation of Cr(VI) is needed. The aim of this work was to evaluate the performance of Cr(VI) reduction using ceramic pearl as a supporting medium in a fixed biofilm reactor. A kinetic model system was developed and verified using the column test. The effluents of Cr(VI) concentration and Cr(III) production were evaluated and compared by the modeling and experimental results. In addition, the growth of attached and suspended *E. coli* cells was determined during the continuous-flow column test. Furthermore, the flux of Cr(VI) into biofilm and the concentration profiles of Cr(VI) at different operation time were evaluated. The study was done at the environmental microbiology laboratory in Taichung of Taiwan from August 2008 to July 2009.

Kinetic model

Reaction stoichiometry

The reaction stoichiometry of simultaneous Cr(VI) reduction and organic acids (as acetic acid) utilization by *E. coli* cells in an anaerobic fixed biofilm reactor is suggested as follows (Chirwa and Wang 2000):

$$CH_3COO^- + 1.5CrO_4^{2-} + 6.5H^+ \rightarrow 1.5Cr^{3+} + 2HCO_3^- + 2H_2O + 1.75H_{2(aq)} \quad (1)$$

Based on the above reaction stoichiometry, the *E. coli* cells used acetate as an electron donor and Cr(VI) as an electron acceptor for their growth. The *E. coli* cells reduced Cr(VI) to form Cr(III).

Model development

The basic assumptions of the model system include, they are as follows: (1) the ceramic pearls are spherical in shape; (2) the biofilm is homogeneous and the density of the biofilm is constant; (3) there is no adsorption on ceramic pearl; (4) no inhibition on *E. coli* 33456 occurred from Cr(VI) concentration; (5) mass transfer phenomenon of Cr(VI) in biofilm is dominated by diffusion based on Fick's law; (6) acetate as electron donor for *E. coli* 33456 growth is a non-limiting substrate; and (7) Cr(VI) as electron acceptor for *E. coli* 33456 growth is a single species for both diffusion and reduction limiting in the biofilm. Figure 1 shows the conceptual basis of a biofilm attached on ceramic pearl.

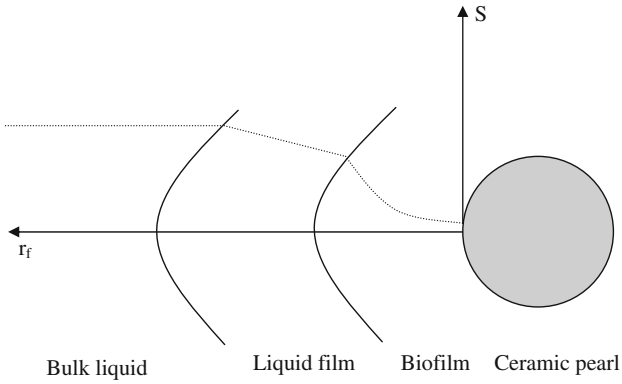

Fig. 1 Cr(VI) concentration profile distributed in fixed biofilm reactor

The governing equations for the Cr(VI) concentration in the liquid phase of a completely mixed, packed-bed reactor were described as follows (Chang and Rittmann 1987):

$$\frac{dS_b}{dt} = \frac{Q}{V\varepsilon}(S_{b0} - S_b) - k_f(S_b - S_s)\frac{A_f}{V\varepsilon} - \frac{kS_b}{K_s + S_b}X_b \quad (2)$$

$$\frac{dX_b}{dt} = \left(\frac{YkS_b}{K_s + S_b} - b - \frac{Q}{V\varepsilon}\right)X_b + \frac{A_f}{V\varepsilon}b_s L_f X_f \quad (3)$$

where S_b is the Cr(VI) concentration in the bulk liquid ($M_s\ L^{-3}$); S_{b0} is the Cr(VI) concentration in the feed ($M_s\ L^{-3}$); S_s is the Cr(VI) concentration at liquid/biofilm interface ($M_s\ L^{-3}$); X_b is the concentration of suspended *E. coli* cells in the bulk liquid ($M_s\ L^{-3}$); k_f is the film transfer coefficient ($L\ T^{-1}$); k is the maximum specific reduction rate of Cr(VI) ($M_s\ M_x\ T^{-1}$); Y is the growth yield of *E. coli* cells ($M_x\ M_s^{-1}$); b_s is the specific shear-loss coefficient of *E. coli* biofilm (T^{-1}); Q is the flow rate of the feed solution ($L^3\ T^{-1}$); V is the effective volume of reactor (L^3); A is the total surface area of media (L^2); and ε is the bed porosity of the reactor. The non-steady state form of mass transfer diffusion across the liquid–biofilm interface and reduction in the biofilm for Cr(VI) can be described by Fick's law and Monod kinetics (Tsai et al. 2005):

$$\frac{\partial S_f}{\partial t} = \frac{D_f}{r_f^2}\frac{\partial}{\partial r_f}\left(r_f^2\frac{\partial S_f}{\partial r_f}\right) - \frac{kS_f}{K_s + S_f}X_f \quad (4)$$

where S_f is the Cr(VI) concentration in the biofilm ($M_s\ L^{-3}$); D_f is the diffusion coefficient of Cr(VI) in the biofilm ($L^2\ T^{-1}$); and r_f is the radial distance in the biofilm (L). Equation (4) requires two boundary conditions. First, the slope of the Cr(VI) concentration at the surface of a supporting medium must be zero. Second, the flux entering the interface from the liquid film must be equal to the flux leaving the interface into the biofilm.

The Cr(VI) diffusing into biofilm can be reduced by *E. coli* cells for biosynthesis. The *E. coli* cells can increase with time until the cells growth rate reaches a steady-state condition. Concerning the biofilm thickness, the major enhancing factors include the cell growth, shear loss from liquid flow, and self-loss of *E. coli* cells. Its temporal variation can be described by the following equation (Liang et al. 2007):

$$\frac{\mathrm{d}(L_\mathrm{f})}{\mathrm{d}t} = \frac{\int_0^{L_\mathrm{f}} \left(\frac{Y_k S_\mathrm{f} X_\mathrm{f}}{K_\mathrm{s}+S_\mathrm{f}}\right) 4\pi r_\mathrm{f}^2 \mathrm{d}r_\mathrm{f}}{A_\mathrm{f} X_\mathrm{f}} - (b + b_\mathrm{s}) L_\mathrm{f} \tag{5}$$

where L_f is the biofilm thickness (L); and A_f is the total surface area of a ceramic pearl (L^2). To compute the concentration of Cr(III) produced from the reduction of Cr(VI) by *E. coli* cells, a mass balance for Cr(III) must be formulated according to the Cr(III) effluent concentration, and the net fluxes of Cr(VI) reduced to Cr(III) by the attached *E. coli* cells as well as the Cr(VI) concentration in the bulk liquid was reduced to Cr(III) by the suspended *E. coli* cells. The Cr(III) production can be described as the following equation

$$\frac{\mathrm{d}C_\mathrm{p}}{\mathrm{d}t} = \frac{Q}{V\varepsilon}\left(-C_\mathrm{p}\right) + \frac{\alpha A_\mathrm{f} k_\mathrm{f}}{V\varepsilon}(S_\mathrm{b} - S_\mathrm{s})(1-Y) + \alpha(1-Y)\frac{kS_\mathrm{b}}{K_\mathrm{s}+S_\mathrm{b}} X_\mathrm{b} \tag{6}$$

where C_p is the Cr(III) concentration in bulk liquid and α is the conversion factor for the reduction of Cr(VI) to Cr(III). A quantity for Cr(VI) flux is important for the understanding of the fixed biofilm process. This quantity is easily computed using the orthogonal collocation method (OCM) solution. Since the Cr(VI) flux from the bulk liquid phase into the biofilm is linear, the flux is easily computed with

$$J_\mathrm{f} = k_\mathrm{f}(S_\mathrm{b} - S_\mathrm{s}) \tag{7}$$

where J_f is the flux of Cr(VI) from bulk liquid into *E. coli* biofilm ($\mathrm{M}_s\ \mathrm{L}^{-2}\ \mathrm{T}^{-1}$).

Model solution

One partial differential equation with four ordinary differential equations in this model can be simplified and made dimensionless by defining dimensionless variables. The Legendre polynomials (even function) were used to approximate the exact Cr(VI) concentration profile in the liquid film and biofilm. The roots of the Legendre polynomials were used as the collocation points. The number of internal collocation points in the biofilm was fixed at 9. The dimensionless partial differential equations can be converted into nine ordinary differential equations by orthogonal collocation method. All of the computer programs were coded in Fortran language and run using a Fortran complier in a Quadra 840 Macintosh computer at the computer laboratory of Central Taiwan University of Science and Technology (Taichung, Taiwan).

Materials and methods

Supporting media

To verify the model system, the ceramic pearl with the diameter 0.6 cm was chosen as the supporting media for biofilm attachment because they are inert media and have an accurately known surface area for *E. coli* cells attachment.

E. coli 33456 culture inoculum

Escherichia coli ATCC 33456 was originally purchased from the American Type Culture Collection (ATCC) and has been in our laboratory collection since 2006. The *E. coli* culture used in all experiments was prepared by washing the harvested *E. coli* cells three times in 0.85 % NaCl solution and then re-suspended and obtained through gradient centrifugation in a modified basal mineral medium supplemented with trace metal and vitamin solutions (Chirwa and Wang 2000). The mineral salt medium for *E. coli* culture was similar as described by Chirwa and Wang (2000). The mineral salt medium for *E. coli* culture was prepared by dissolving (per liter): NH_4Cl, 1.013 g; $NaH_2PO_4{\cdot}2H_2O$, 0.62 g; K_2HPO_4, 2.5 g; $MgSO_4{\cdot}7H_2O$, 0.0103 g; $CaCl_2{\cdot}2H_2O$, 0.00425 g; $FeCl_3{\cdot}3H_2O$ 0.00085 g. The trace metal stock solution contained $FeCl_3{\cdot}6H_2O$, 0.243 g; $MnCl_2{\cdot}2H_2O$ 0.06 g; $ZnCl_2$, 0.041 g; $CuCl_2{\cdot}2H_2O$ 0.036 g; $CoCl_2{\cdot}2H_2O$, 0.036 g; $Na_2B_4O_7{\cdot}10H_2O$, 0.015 g; Na_3-Citrate, 2.205 g; $(NH_4)_6Mo_7O_{27}{\cdot}4H_2O$, 0.026 g; KH_2PO_4, 5.104 g; $NaH_2PO_4{\cdot}H_2O$, 3.105 g; $(NH_4)_2SO_4$, 1.980 g; NH_4Cl, 18.450 g; $CaCl_2{\cdot}2H_2O$, 2.205 g; $MgCl_2{\cdot}6H_2O$, 3.049 g; $NiCl_2{\cdot}6H_2O$, 0.025 g in 1 L of deionized water; along with 5 mL of a trace vitamin B_{12} stock solution. The 5.0 mM sodium acetate was added as an electron donor for *E. coli* growth in the mineral salt medium. A sterilized stock solution of potassium chromate (K_2CrO_4) was prepared for the use of Cr(VI). *E. coli* cells were harvested during the log growth phase in nutrient broth after incubation at 35 °C for 16 h.

Continuous-flow column test

The reactor was inoculated by charging a 75 mL *E. coli* with 4.5 mg cell/L. An anaerobic fixed biofilm reactor with a high recycle flow rate ($Q_\mathrm{r}/Q = 30$) for maintaining a completely mixed stirred tank reactor (CSTR) was applied to conduct the experiments of Cr(VI) reduction. Into the

reactor was fed an Cr(VI) at an initial concentration of 5 mg Cr(VI)/L with mineral salt medium at 720 cm^3/day. The reactor volume was 320 cm^3, which yielded a hydraulic retention time (HRT) of 10.7 h. The reactor temperature was maintained at 35 ± 0.1 °C using a circulating water bath (Yih Der Inc., Taipei, Taiwan) for water jacket of the bioreactor. The ceramic pearls were placed in the reactor zone between two plates used for fixation. Earlier work has shown that Cr(VI) reduction by *E. coli* cells was inhibited in the presence of oxygen (Shen and Wang 1994). The test column was purged using 99.999 % nitrogen gas filtered by a Whatman glass filter to establish an anaerobic condition for the experiments. The pH was buffered at 7.1 ± 0.2 by adding $HPO_4^{2-}/H_2PO_4^-$ in the feed solution (Nkhalambayausi-chirwa and Wang 2001). Figure 2 depicts the laboratory-scale experimental setup of the fixed biofilm reactor for Cr(VI) reduction.

Measurement of *E. coli* biofilm density

E. coli biofilm grown on ceramic pearls was used to measure biofilm density. At the end of the column test, 150 ceramic pearls with biofilm were transferred, one by one with tweezer to preclude the inclusion of interstitial water, to a tared aluminum pan. The ceramic beads containing *E. coli* biofilm were weighed before and after drying in the oven to determine the *E. coli* biofilm mass. Clean ceramic pearls were immersed in clean water and picked out to measure the amount of attached water on ceramic pearls by the same methods. The *E. coli* biofilm volume was obtained by calculating the difference of the two measurements. The density of *E. coli* biofilm thus computed by dividing the biofilm mass by biofilm volume was 0.836 mg cell/mL.

Analytical methods

Cr(VI) content was determined spectrophotometrically at 540 nm using a UV–Vis spectrophotometer (Shimadzu, model UV-1700), following the colorimetric method with 1,5-diphenyl-carbazide in acid solutions, as described in Section 3500 B of the Standard Methods (APHA 2005). The concentration of Cr(III) was measured using an ICS 1500 Ion Chromatograph system (Dionex Corporation, Sunny-vale, CA) that was equipped with an HPIC-CS5 column and quantified at 520 nm using a UV–Vis detector (Wang and Shen 1997; Chirwa and Wang 2000). All tests were duplicated, and the relative experimental error of Cr(VI) analysis was estimated to be within ±5 %. The optical density of the *E. coli* cells suspension was determined by turbidimetric measurement in a UV–Vis spectrophotometer (Shimadzu, model UV-1700) at 610 nm and correlated to dry cell weight (Wang and Shen 1997; Bae et al. 2000).

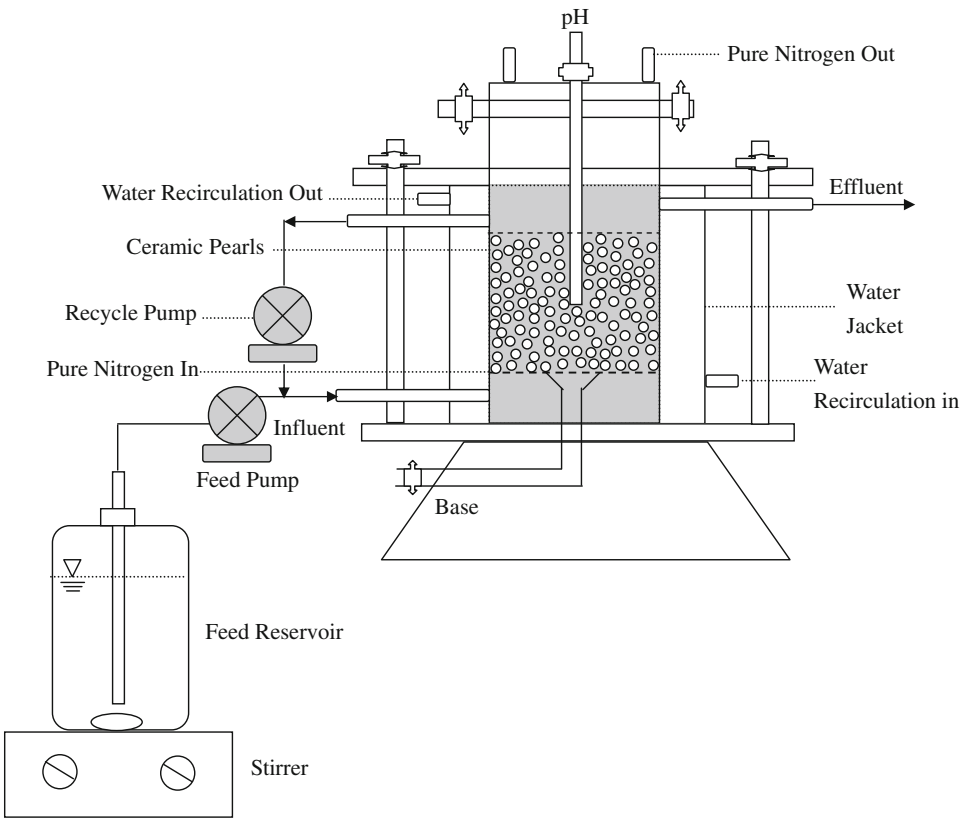

Fig. 2 Experimental setup for *E. coli* cells biofilm model verification

Results and discussion

Determination of biokinetic parameters

Figure 3 depicts the experimental data on the variations of Cr(VI) and suspended *E. coli* cells versus operation time. It can be observed that the experimental data of the suspended *E. coli* cells represent a typical growth and decay curve with a well-defined growth phase, followed by a constant growth phase and the endogenous phase (Pirbazari et al. 1996). The experimental data of Cr(VI) and suspended *E. coli* cells concentrations facilitate a priori estimation of biokinetic parameters by evaluating the growth rate of suspended *E. coli* cells and Cr(VI) reduction. The relevant techniques employed for the determination of biokinetic parameters from the experimental data of the batch test are discussed as follows.

Escherichia coli cells are responsible for Cr(VI) reduction in this anaerobic fixed biofilm process. To predict the performance of an anaerobic fixed biofilm process correctly, the batch suspended-growth kinetic tests were used to determine four biokinetic coefficients, namely the Monod maximum specific reduction rate of Cr(VI) (k), Monod half-velocity coefficient (K_s), growth yield for *E. coli* cells (Y), and the decay coefficient (b) for *E. coli* cells, respectively.

A batch test with Cr(VI), acetate, and suspended *E. coli* cells was conducted to determine the biokinetic parameters. The initial Cr(VI) and suspended *E. coli* cells concentration were 10 mg Cr(VI)/L and 8 mg cell/L, respectively. The yield coefficient (Y) of *E. coli* cells was approximately constant over the range of Cr(VI) concentration encountered in the growth phase. Under these circumstances, the growth yield for *E. coli* cells can be expressed by:

$$Y = -\frac{\Delta X}{\Delta S} \tag{8}$$

where ΔX is the increase in *E. coli* cells concentration and ΔS is the change in Cr(VI) concentration. The growth yield for *E. coli* cells was determined from the slope shown in Fig. 4. The growth yield for *E. coli* cells was 0.24 mg cell/mg Cr(VI).

The Monod maximum specific growth rate (μ_m) was determined from the slope of the growth curve of *E. coli* cells at the log growth phase in the yield experiment. The following equation was employed to compute μ_m:

$$\mu_m = \frac{\ln(X_t/X_0)}{t} \tag{9}$$

where X_0 and X_t are *E. coli* cells concentration at time zero and t. The Monod maximum specific growth rate of *E. coli*

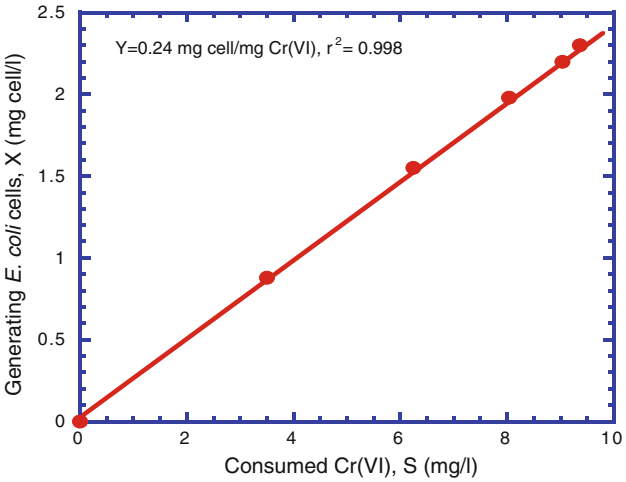

Fig. 4 Batch kinetic test to determine growth yield (Y) for *E. coli* cells

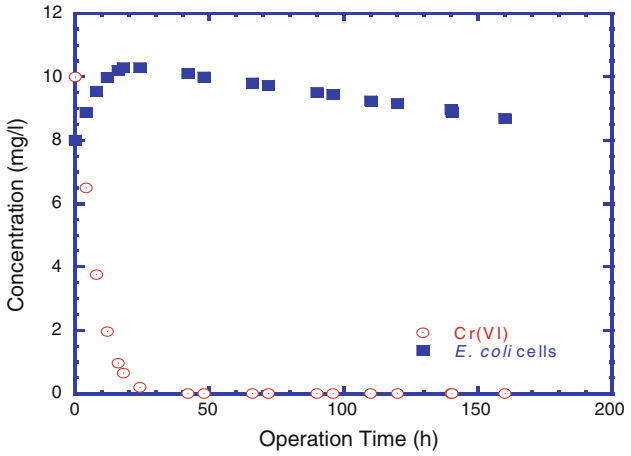

Fig. 3 Batch kinetic test for Cr(VI) reduction and the growth of *E. coli* cells

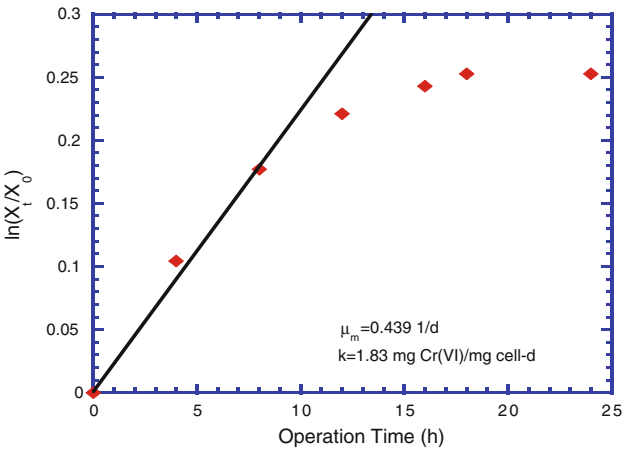

Fig. 5 Batch kinetic test to determine Monod maximum specific growth rate (μ_m) and Monod maximum specific utilization rate (k) for *E. coli* cells

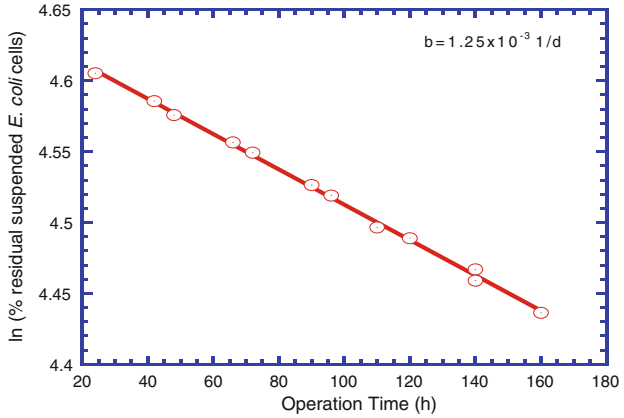

Fig. 6 Batch kinetic test to determine decay coefficient (b) for *E. coli* cells

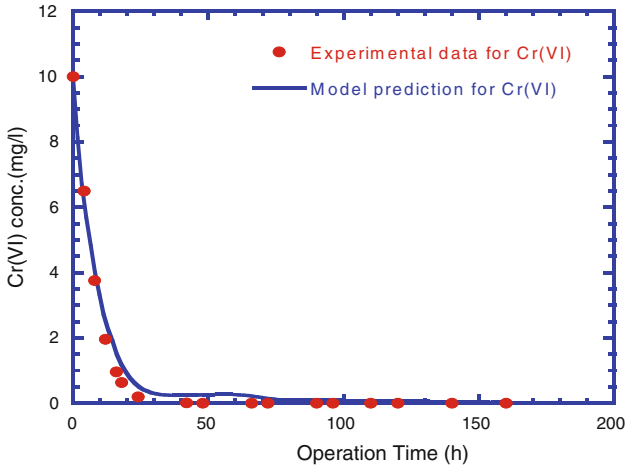

Fig. 7 Comparison of experimental data and model prediction to yield a best-fit value of Monod half-velocity coefficient of Cr(VI) (K_s)

cells, as depicted in Fig. 5, was equal to 0.439 day^{-1}. The k value can be computed by μ_m/Y. The k value for *E. coli* cells was 1.83 mg Cr(VI)/mg cell-day.

The concentration data of *E. coli* cells in the endogenous phase were applied to evaluate the decay coefficient (b) of *E. coli* cells. In the endogenous phase, the *E. coli* cells concentration was decreased with time and the decay coefficient (b) was determined from the slope of a linearized plot of ln$X$ versus time shown in Fig. 6. The decay coefficient (b) can be represented by the following equation:

$$b = \frac{\ln(X_0/X_t)}{t} \tag{10}$$

where X_0 and X_t are biomass at time zero and t, respectively. The decay coefficient for *E. coli* cells was 1.25×10^{-3} 1/day.

Once the yield growth of *E. coli* cells (Y), Monod maximum specific utilization rate of Cr(VI) (k), and the decay coefficient of *E. coli* cells (b) were determined from the slopes of growth and endogenous phrases, respectively, in the batch kinetic test, then the Cr(VI) reduction rate with the growth rate of suspended *E. coli* cells described by Monod kinetics was used to determine the value of the Monod half-velocity coefficient of Cr(VI) (K_s). The Cr(VI) reduction rate with the growth rate of suspended *E. coli* cells can be represented by the following Eqs. (11)–(12), respectively (Ucun et al. 2010):

$$\frac{dS}{dt} = -\frac{kXS}{K_s + S} \tag{11}$$

$$\frac{dX}{dt} = \left(\frac{YkS}{K_s + S} - b\right)X \tag{12}$$

where S is the concentration of Cr(VI) (M_s L^{-3}) and X is the concentration of *E. coli* cells (M_x L^{-3}).

Batch kinetic test was conducted to obtain the experimental result of Cr(VI) concentration versus time. The predicted Cr(VI) concentration versus time is determined using the suspended *E. coli* kinetic model by assuming K_s value for model prediction. A best-fit K_s value was obtained by minimizing the sum of least-square value (LSV) between and the experimental and the predicted results for Cr(VI) reduction from the batch test (Liang et al. 2007):

$$\text{LSV} = \frac{1}{N}\sum_{i=1}^{N}\sqrt{\frac{(S_{\text{pre},i} - S_{\text{exp},i})^2}{(S_{\text{exp},i})^2}} \tag{13}$$

where $S_{\text{pre},i}$ and $S_{\text{exp},i}$ are Cr(VI) concentration of model prediction and experimental data, respectively. N is the number of data point. The least-square value (LSV) provides a quantitative comparison of the agreement between the predicted and the experimental data. As the LSV increases, the level of agreement between the model prediction and the experimental data decreases. The experimental data and the model prediction for Cr(VI) reduction are plotted in Fig. 7. The best-fit K_s value for Cr(VI) was 14.8 mg Cr(VI)/L.

Determination of mass transfer coefficients

Diffusion coefficients in biofilm are generally less than those in the liquid phase due to the diffusional resistance to the transport of the chemical species, which is posed by bacteria and their extracellular materials. Therefore, the diffusion coefficient in the biofilm is obtained by multiplying the diffusion coefficient in the bulk liquid phase (D_w) by a factor of 0.8 to correct the additional diffusional resistance in the biofilm (Williamson and McCarty 1976). Lazaridis and Charalambous (2005) found that the diffusion coefficient of Cr(VI) in bulk liquid has a mean value of 2.1×10^{-10} m^2/s (0.18 cm^2/day), which was applied as

Table 1 Reactor and biokinetic parameters used for model prediction

Symbol	Parameter description (unit)	Value	Remarks
S_{b0}	Cr(VI) concentration in the feed (mg Cr(VI)/L)	5	Measured
k	Maximum specific reduction rate of Cr(VI) (mg Cr(VI)/mg cell-day)	1.83	Measured
Y	Growth yield of *E. coli* cells (mg cell/mg Cr(VI))	0.24	Measured
K_s	Monod half-velocity coefficient of Cr(VI) (mg Cr(VI)/L)	14.8	Compared
b	Decay coefficient of *E. coli* cells (1/day)	1.25×10^{-3}	Measured
D_f	Diffusion coefficient of Cr(VI) in biofilm (cm^2/day)	0.144	Calculated
k_f	Liquid film transfer coefficient of Cr(VI) (cm/day)	4.144	Calculated
b_s	Specific shear-loss coefficient of *E. coli* biofilm (1/day)	2.3×10^{-3}	Calculated
X_f	Density of *E. coli* biofilm (mg cell/mL)	0.836	Measured
X_{s0}	Concentration of suspended *E. coli* in the feed (mg cell/mL)	4.5×10^{-3}	Measured
L_{f0}	Initial *E. coli* biofilm thickness (μm)	5.5	Assumed
V	Effective working volume	320	Measured
Q	Influent flow rate (mL/day)	720	Measured
ε	Reactor porosity	0.87	Measured
α	Conversion factor for the reduction of Cr(VI) to Cr(III) (mg Cr(III)/mg CrO_4^{2-})	0.45	Calculated
d_p	diameter of ceramic pearl (cm)	0.6	Measured
A_f	Total surface area of ceramic pearl (cm^2)	2,787	Calculated

D_w in this study. Thus, the computed value of molecular diffusion coefficient for Cr(VI) in the biofilm was equal to 0.144 cm^2/day.

The film transfer coefficient (k_f) computed from the empirical formula for the packed-bed reactor was described in the following equation (Cussler 1984):

$$k_f = 1.17 v_s (R)^{-0.42} (S)^{-0.67} \quad (14)$$

where v_s is the superficial flow velocity through column (L T^{-1}); R is the Reynolds number $= \frac{d_p v_s}{v}$; S is the Schmidt number $= \frac{v}{D_w}$; d_p is the diameter of the ceramic pearl (L); and v is the kinematic viscosity (L^2 T^{-1}). The computed value of film transfer coefficient for Cr(VI) was equal to 4.144 cm/day.

An empirical formula suitable for spherical particle was used to evaluate specific shear-loss coefficient (b_s) of the *E. coli* biofilm on the ceramic pearl (Speitel Jr. and DiGiano 1987). The value of b_s was calculated from the following equation:

$$b_s = 2.29 \times 10^{-6} \left[\frac{\mu v_s (1-\varepsilon)^3}{d_p^2 \varepsilon^3 a} \right]^{0.58} \quad (15)$$

where μ is the viscosity of water (M_s L^{-1} T^{-1}); and a is the specific surface area of bed (L^{-1}). The computed value of b_s was equal to 2.3×10^{-3} day^{-1}. Moreover, the conversion factor for the reduction of Cr(VI) to Cr(III) was equal to 0.45 mg Cr(III)/mg Cr(VI) according to the reaction stoichiometry.

Cr(VI) reduction and Cr(III) production

The kinetic model was verified by investigating Cr(VI) reduction by conducting a column test fed with 5 mg Cr(VI)/L and mineral salt medium. The reactor and biokinetic parameters obtained from the batch kinetic test were used for model prediction are listed in Table 1. Figure 8a presents the Cr(VI) effluent concentration varied with time. The effluent curve of Cr(VI) concentration can be described in three parts. First, the Cr(VI) concentration increased sharply to approximately 2.7 mg Cr(VI)/L (0.53 S_{b0}) at the first day. There was no significant reduction of Cr(VI) during the period of 5 days. Second, the *E. coli* biofilm was vigorously reducing Cr(VI) for the transient period at 5–25 days. During this period, the Cr(VI) concentration rapidly decreased due to the significant growth of *E. coli* biofilm. The third part of the effluent of Cr(VI) concentration ranging from 25 to 146 days ran at a steady-state condition. The effluent Cr(VI) concentration was around 0.39 mg Cr(VI)/L (0.078 S_{b0}) when the *E. coli* biofilm and suspended *E. coli* cells reached a maximal growth at a steady-state condition. The removal efficiency of Cr(VI) was about 92 % at a steady-state condition. The least-square value (LSV) for Cr(VI) reduction was 0.174.

To verify Cr(VI) reduction in fixed-bed reactor, production of Cr(III) was observed in this test. The production of Cr(III) varied with time presented in Fig. 8b. The Cr(III) concentration at the steady state was approximately 1.6 mg/L (0.32 S_{b0}). The model-predicted concentration of Cr(III) maintained the same trend with the experimental

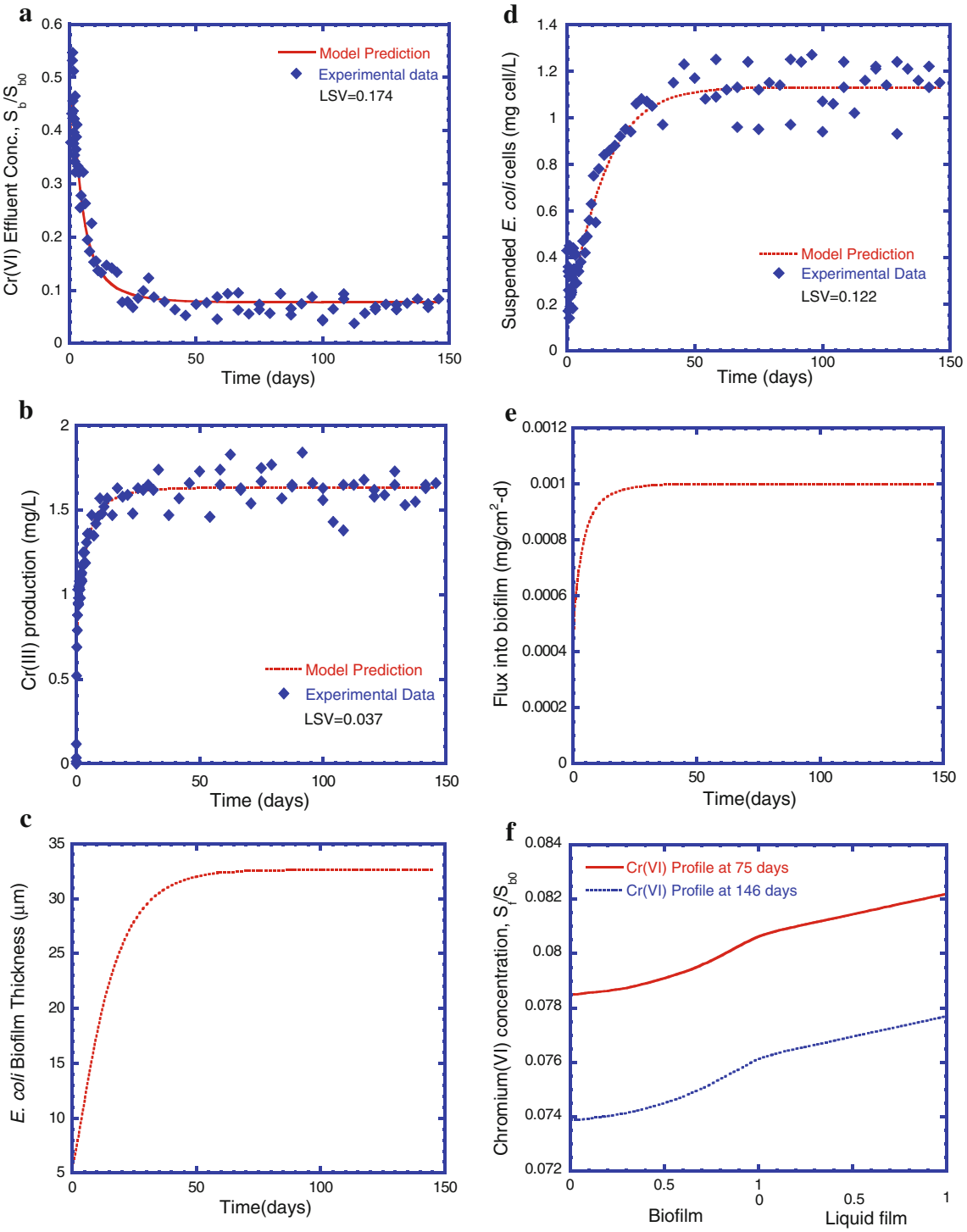

Fig. 8 Experimental data and model prediction **a** Cr(VI) effluent, **b** Cr(III) production, **c** *E. coli* biofilm growth curve, **d** suspended *E. coli* cells growth curve, **e** flux into *E. coli* biofilm, **f** Cr(VI) concentration profiles in *E. coli* biofilm

result after 20 days. The model simulation is fair agreement with the experimental results because a moderate least-square value (LSV) of 0.037 was obtained. Approximately 33 % of Cr(VI) was converted to Cr(III) at a steady-state condition.

Growth of *E. coli* cells

Figure 8c shows the growth curve of *E. coli* biofilm varied with time. There was no elapsed time required for *E. coli* biofilm to start to grow. *E. coli* biofilm is vigorously

reducing Cr(VI) at a transient period of 40 days. Then, *E. coli* biofilm thickness reached a maximum value of 32.6 μm at a steady-state condition from day 40 to day 146 while Cr(VI) was vigorously reduced by *E. coli* biofilm.

One indicator of the generating cells growth was the concentration of suspended *E. coli* cells in the effluent. The general trend of the suspended *E. coli* cells concentration in effluent by model prediction was similar to the experimental data obtained from completely mixed continuous-flow column test, as depicted in Fig. 8d. Good agreement existed between the model prediction and the experimental data for suspended *E. coli* cells growth in the fixed biofilm reactor owing to low least-square value (LSV) of 0.122. The growth curves of *E. coli* biofilm and suspended *E. coli* cells presented the same trend of variation with time, which indicated attached and suspended *E. coli* cells bio-reduced Cr(VI) simultaneously in the fixed biofilm reactor. The log growth rate during 20 days represented that the suspended *E. coli* cells actively bio-reduced Cr(VI). At the steady state, the concentration of suspended *E. coli* cells was approximately 1.2 mg cell/L.

Cr(VI) flux into biofilm

Figure 8e presents the model-predicted Cr(VI) flux diffusing from bulk liquid into biofilm. Cr(VI) flux represents *E. coli* biofilm reduction. At the beginning of the test, the Cr(VI) flux started out at zero as *E. coli* biofilm growth was negligible. The Cr(VI) flux increased abruptly as the *E. coli* biofilm grew at logarithmic rate during 40 days. During this period, the *E. coli* biofilm thickened and consumed Cr(VI) vigorously in the fixed biofilm reactor. Thus, the difference in Cr(VI) concentration in bulk liquid and the biofilm/liquid interface increased, which significantly increased the Cr(VI) flux into biofilm due to reduction activity. During 5–10 days, the Cr(VI) concentration in effluent continued to decrease and then reached a constant concentration under a steady-state condition. The Cr(VI) flux reached a constant value and remained maximal, which was about 1×10^{-3} mg/cm^2 day.

Concentration profiles of Cr(VI)

The Cr(VI) concentration profiles in liquid film and biofilm at 75 and 146 days are shown in Fig. 8f. The Cr(VI) diffused through the liquid film into *E. coli* biofilm to form a concentration profile due to diffusional resistance. The Cr(VI) concentration profiles at 75 and 146 days exist the similar trends because both the concentration profiles were determined at the steady state. The *E. coli* biofilm at 75 and 146 days was 32.6 μm at a steady-state period. The biofilm at this stage could be called a "shallow" biofilm (Suidan et al. 1987).

Conclusion

The model system was derived to describe the Cr(VI) reduction using ceramic pearl as a supporting medium in a fixed biofilm reactor. Experimental results demonstrate that the fixed biofilm process is able to reach a high removal efficiency for Cr(VI) reduction. With assumed values of initial biofilm thickness (L_{f0}), the mathematical model simulated fairly well the experimental results for the Cr(VI) effluent concentration, effluent concentration of suspended *E. coli,* and Cr(III) production. Attached and suspended *E. coli* cells simultaneously reduced Cr(VI) and approached a maximum growth at the steady state. The Cr(VI) flux diffusing from bulk liquid into biofilm increased rapidly as *E. coli* biofilm grew vigorously during the transient-state period. The effluent concentration of Cr(III) at a steady-state condition was approximately 1.6 mg/L. The approaches of modeling and experiments used in this study can be applied to scale up the fixed biofilm reactor to treat Cr(VI)-containing wastewater.

Acknowledgments The author would like to thank the National Science Council of Taiwan for partially supporting this research under Contract No. NSC 96-2221-E-166-004-MY2. Ted Knoy is appreciated for his editorial assistance.

Nomenclatures

μ	Viscosity of water ($M_s\ L^{-1}\ T^{-1}$)
a	Specific surface area of bed (L^{-1})
A_f	Total surface area of ceramic pearl (L^2)
b	Decay coefficient of *E. coli* cells (T^{-1})
b_s	Shear-loss coefficient of *E. coli* cells (T^{-1})
C_p	Concentration of Cr(III) in bulk liquid ($M_s\ L^{-3}$)
D_f	Diffusion coefficient of Cr(VI) in biofilm ($L^2\ T^{-1}$)
d_p	Diameter of ceramic pearl (L)
D_w	Diffusion coefficient in the bulk liquid phase ($L^2\ T^{-1}$)
J_f	Flux of Cr(VI) from bulk liquid into *E. coli* biofilm ($M_s\ L^{-2}\ T^{-1}$)
k	Monod maximum specific reduction rate of Cr(VI) ($M_s\ M_x\ T^{-1}$)
k_f	Liquid film transfer coefficient of Cr(VI) ($L\ T^{-1}$)
K_s	Monod half-velocity coefficient of Cr(VI) ($M_s\ L^{-3}$)
L_f	Biofilm thickness (L)
L_{f0}	Initial biofilm thickness (L)
M_s	Mass of chromium
M_x	Mass of *E. coli* cells
Q	Influent flow rate ($L^3\ T^{-1}$)
r_f	Radial distance in biofilm (L)

S_b	Concentration of Cr(VI) in bulk liquid ($M_s\ L^{-3}$)
S_{b0}	Concentration of Cr(VI) in feed ($M_s\ L^{-3}$)
S_f	Concentration of Cr(VI) in biofilm ($M_s\ L^{-3}$)
S_s	Concentration of Cr(VI) at liquid/biofilm interface ($M_s\ L^{-3}$)
t	Time (T)
V	Effective working volume of reactor (L^3)
v_s	Superficial flow velocity through column ($L\ T^{-1}$)
X_b	Density of *E. coli* cells in bulk liquid ($M_x\ L^{-3}$)
X_{b0}	Density of *E. coli* cells in feed ($M_x\ L^{-3}$)
X_f	Density of *E. coli* cells in biofilm ($M_x\ L^{-3}$)
Y	Growth yield of *E. coli* cells ($M_x\ M_s^{-1}$)
α	Conversion factor for the reduction of Cr(VI) to Cr(III) ($M_s\ M_s^{-1}$)
ε	Reactor porosity (dimensionless)
μ_m	Monod maximum specific growth rate (T^{-1})
υ	Kinematic viscosity ($L^2\ T^{-1}$)

References

American Public Health Association (2005) Standard methods for the examination of water and wastewater, 21st edn. APHA, Washington, DC

Bae WC, Kang TG, Kang IK, Won YJ, Jeong BC (2000) Reduction of hexavalent chromium by *Escherichia coli* ATCC 33456 in batch and continuous cultures. J Microbiol 38(1):36–39

Baran A, Biçak E, Baysal SH, Önal S (2007) Comparative studies on the adsorption of Cr(VI) ions on to various sorbents. Bioresour Technol 98(3):661–665

Chang HT, Rittmann BE (1987) Mathematical modeling of biofilm on activated carbon. Environ Sci Technol 21(3):273–279

Chirwa EN, Wang YT (2000) Simultaneous chromium(VI) reduction and phenol degradation in an anaerobic consortium of bacteria. Water Res 34(8):2376–2384

Cussler EL (1984) Diffusion: mass transfer in fluid systems, 2nd edn. Cambridge University Press, New York

Goyal N, Jain SC, Banerjee UC (2003) Comparative studies on the microbial adsorption of heavy metals. Adv Environ Res 7(2):311–319

Kanmani P, Aravind J, Devasia P (2012) Remediation of chromium contaminants using bacteria. Int J Environ Sci Tech 9(1): 463–472

Lazaridis NK, Charalambous Ch (2005) Sorptive removal of trivalent and hexavalent chromium from binary aqueous solutions by composite alginate-goethite beads. Water Res 39(18):4385–4396

Liang CH, Chiang PC, Chang EE (2007) Modeling the behaviors of adsorption and biodegradation in biological activated carbon filters. Water Res 41(15):3241–3250

Lovley DR, Phillips EJP (1994) Reduction of chromate by *Desulfovibrio vulgaris* and its c3 cytochrome. Appl Environ Microbiol 60(2):726–728

Nkhalambayausi-chirwa EM, Wang YT (2001) Simultaneous chromium(VI) reduction and phenol degradation in a fixed-film coculture bioreactor: reactor performance. Water Res 35(8):1921–1932

Pirbazari M, Ravindran V, Badriyha BN (1996) Hybrid membrane filtration process for leachate treatment. Water Res 30(11): 2691–2706

Shen H, Wang YT (1994) Modeling hexavalent chromium reduction in *E. coli* 33456. Biotechnol Bioeng 43(4):293–300

Speitel Jr GE, DiGiano FA (1987) Biofilm shearing under dynamic conditions. J Environ Eng ASCE 113(3):464–475

Suidan MT, Rittmann BE, Traegner UK (1987) Criteria establishing biofilm-kinetic types. Water Res 21(4):491–498

Tsai HH, Ravindran V, Pirbazari M (2005) Model for predicting the performance of membrane bioadsorber reactor process in water treatment applications. Chem Eng Sci 60(20):5620–5636

Ucun H, Yildiz E, Nuhoglu E (2010) Phenol biodegradation in a batch jet loop bioreactor (JLB): kinetic study and pH variation. Bioresour Technol 101(9):2965–2971

Wang YT, Chirwa EM (1998) Simultaneous removal of Cr(VI) and phenol in chemostat culture of *E. coli* ATCC 33456 and *P. putida* DMP-1. Water Sci Technol 38(8–9):113–119

Wang YT, Shen H (1997) Modelling Cr(VI) reduction by pure bacterial cultures. Water Res 31(4):727–732

Wang YT, Xiao C (1995) Factors affecting hexavalent chromium reduction in pure cultures of bacteria. Water Res 29(11):2467–2474

Williamson K, McCarty PL (1976) Verification studies of the biofilm model for bacterial substrate utilization. J Water Pollut Control Fed 48(2):281–296

Yassi A, Nieboer E (1988) Carcinogenicity of chromium compounds. In: Nriagu JO, Nieboer E (eds) Chromium in natural and human environments. Wiley-Interscience, New York, pp 443–495